Journal of Catalysis **205,** 1–6 (2002)
doi:10.1006/jcat.2001.3430, available online at http://www.idealibrary.com on IDEAL®

PRIORITY COMMUNICATION

Atomic Scale Observations of the Chemistry at the Metal–Oxide Interface in Heterogeneous Catalysts

R. F. Klie,*[,1] M. M. Disko,† and N. D. Browning*

**Department of Physics (M/C 273), University of Illinois at Chicago, 845 West Taylor Street, Chicago, Illinois 60607-7059; and †Corporate Strategic Research, ExxonMobil Research and Engineering, Annandale, New Jersey 08801*

Received July 27, 2001; revised September 27, 2001; accepted October 4, 2001

Here we present a preliminary analysis of the atomic scale interface chemistry in a model heterogeneous catalyst system, Pt/SiO_2. We show that the combination of Z-contrast imaging and electron energy loss spectroscopy (EELS) in the scanning transmission electron microscope (STEM) exhibits a sensitivity to surface oxidation and changes in the interfacial chemistry that is higher than that of conventional analytical methods such as energy-dispersive X-ray spectroscopy (EDS), chemisorption, and X-ray absorption near edge structure analysis (XANES). In particular, the presence of a few monolayers of platinum oxide can be clearly seen, and changes in the chemistry of the SiO_2 support within ∼1 nm of the metal–oxide interface can be characterized as a function of the catalyst preparation conditions. These results demonstrate that this combination of novel techniques can provide unparalleled information that is potentially the key to understanding the activity and selectivity of heterogeneous catalyst systems. © 2002 Elsevier Science

Key Words: **STEM; Z-contrast imaging; EELS; heterogeneous catalyst; Pt/SiO_2.**

1. INTRODUCTION

Heterogeneous noble metal catalysts are routinely used in a wide variety of chemical processes, including dehydrogenation, naphtha reforming, oxidation, and automotive exhaust catalysis (for example, see Ref. 1). Although successfully utilized for many years, a fundamental understanding of the mechanism behind their activity and selectivity has been elusive (1–3). Here we describe the use of a combination of Z-contrast imaging (4) and electron energy loss spectroscopy (EELS) (5) in the scanning transmission electron microscope (STEM) that permits the characterization of individual nanoclusters in heterogeneous catalyst systems on the fundamental atomic scale. In this preliminary study, the potential of the technique is illustrated through analysis of the Pt/SiO_2 system.

Due to its widespread applications, Pt/SiO_2 has been investigated previously by surface methods, such as X-ray photoemission spectroscopy (XPS), infrared absorption spectroscopy or chemisorption, and extended X-ray absorption fine structure (EXAFS) (7). However, although accurate information on the electronic structure can be obtained from these techniques, they all lack the ability to define the spatial location from which the information is obtained. Similarly, the recent development of sum frequency generation (SFG) as a powerful tool for surface and interface studies (see for example (8)) over an enormous range of ambient pressures suffers from the same problem.

This lack of spatial resolution is particularly important, as it has become increasingly clear that in many cases the core phenomena occur at interfaces between the metal clusters and the support (9). While the traditional method of investigating interfaces, transmission electron microscopy (TEM) (2, 10), provides a high degree of spatial resolution, it is not sensitive to small local changes in composition and electronic structure. There is therefore an "information gap" between what can be learned from spectroscopy and what can be obtained from microscopy. The combination of Z-contrast imaging and electron energy loss spectroscopy (EELS), can potentially fill this "information gap." The atomic resolution and the sensitivity of the image to the atomic number means that even the smallest cluster (a single atom) on an oxide support can be easily identified (11). Using this image to position the probe, an energy loss spectrum can be acquired from any location in and around the interface (12, 13), allowing local changes in electronic structure to be correlated directly with the size and composition of the metal cluster.

2. EXPERIMENTAL & METHODS

The experimental results presented in this paper were obtained using a JEOL 2010F STEM/TEM (14, 15), having a Schottky FEG-source and being operated at 200 kV. It is

[1] To whom correspondence should be addressed. Fax: 1-312-996-4451. E-mail: rfklie@uic.edu.

0021-9517/02 $35.00
© 2002 Elsevier Science
All rights reserved.

equipped with a standard UHR ("ultra-high-resolution") objective lens pole piece, a JEOL annular dark-field detector, a post-column Gatan imaging filter (GIF) (14, 15). The oxygen partial pressure in the column is 5×10^{-8} Pa. The lens conditions in the microscope were defined for a probe-size of 0.2 nm, with a convergence angle of 13 mrad and a collection angle of 52 mrad. With these settings, the probe current is sufficient (40 pA) to obtain statistically significant information and the Z-contrast image is essentially incoherent; i.e., a direct image of the structure is acquired. Furthermore, if the atomic spacing in a zone-axis orientation is larger than the probe size, an atomic resolution image can be obtained (14–16).

The experimental setup of this microscope allows us to use low-angle scattered electrons that do not contribute to the Z-contrast image for EELS (17). As the two techniques do not interfere, Z-contrast images can be used to position the electron probe at the desired spot in the sample to acquire spectra (5, 13, 16). The physical principle behind EELS relates to the interaction of the fast electrons with the sample to cause either collective excitations of electrons (plasmons), or discrete transitions between atomic energy levels (12, 13).

For Pt and SiO_2 we are primarily interested in the bonding interactions with oxygen. To investigate this, the near-edge fine structure of the oxygen K-edge contains valuable information about the nearest neighbor bonding (O $2p$ with the cation $3p$ (Si) or $5d$ (Pt) and the hybridization with the cation sp band) (12, 13). Furthermore, the silicon transitions from $2p$ to the conduction band, which indicate the number of available orbitals for hybridization with the oxygen bands, also lie in the sensitive part of the energy loss spectrum. The localization of any edge below 100 eV is insufficient to measure local changes in the fine structure at the atomic level and will therefore be disregarded (19). The only localized Pt-edges in the sensitivity range of spectrometer have a delayed edge onset and change only very subtly with chemical environment and will therefore be neglected in this paper.

The *in situ* heating experiments performed here utilize a double tilt heating stage with a miniature, encapsulated heater that can be operated in the temperature range between 20 and 1000°C (for a more detailed description see (20)). This setup allows us to simulate conditions closer to the operating temperatures for most catalysts and observe directly thermally induced changes at the surface and interface structures due to this reduction process. The experimental conditions in the microscope mean that beam damage is always a potential issue. However, for the results obtained here, several spectra are acquired consecutively in each position and compared to ensure that beam damage is not contributing significantly to the observed spectral changes (13). The energy-loss scale of the O K-edges was previously calibrated by using the C core-loss edges on a different part of the sample assuming energy shift during the course of the experiments. The zero-loss peak, present in the low-energy spectra, defined the Si L-edge onsets.

3. SAMPLE PREPARATION

The catalytic systems were prepared by impregnating colloidal amorphous SiO_2 microspheres (Nissan Chemical Snowtex ZL), with a surface area of 35.5 m^2/g and a pore volume of 0.25 cm^3/g, with platinum tetraamminehydroxide (pH 9.3), to achieve a nominal Pt-loading of 1.7%. After overnight drying at 120°C, the resulting Pt/SiO_2 catalyst was exposed to two different calcination treatments.

Pt/SiO_2 (350°C)

The Pt/SiO_2 sample was heated in an oven to a temperature of 350°C in air. The calcination process was completed after 3 h and the catalyst was then prepared for TEM analysis. To achieve the appropriate electron transparent samples, the catalyst was crushed to a fine powder. A pure copper grid was then dipped into the fine crushed powder, and a considerable amount of material stuck to the grid for TEM investigations. We intentionally did not use holey carbon films to avoid carbon contamination during the microscopic analysis. The average metal particle size is measured by conventional phase contrast imaging to be ∼20 nm with a medium average dispersion of ∼4.5%.

Pt/SiO_2 (250°C)

The Pt/SiO_2 system was heated in air from room temperature to 250°C and kept at this temperature for 3 h. The TEM sample was prepared in the same manner as the previous one. Here again we used pure copper grids and low magnification CTEM measurements reveal that the average particle size is ∼15 nm with a dispersion of ∼6%. Both samples were stored and prepared at ambient atmospheres.

4. RESULTS

Pt/SiO_2 (350°C)

Figure 1 shows a room-temperature high-resolution image of a particle edge on the supporting SiO_2 sphere in a random orientation (i.e., atomic resolution images of the lattice are not possible). Related studies showed that the Pt particles are single crystals with a cubic lattice structure. The examination of several edge on particles reveals that the bright core of the particle is surrounded by a darker ring of material which seems to be of a different nature than the center.

Figure 1b shows the O K-edge spectra from positions indicated in Fig. 1a. The sample drift was negligible during the acquisition time, so we can assume the information is acquired only from the area of the initial spot, which we

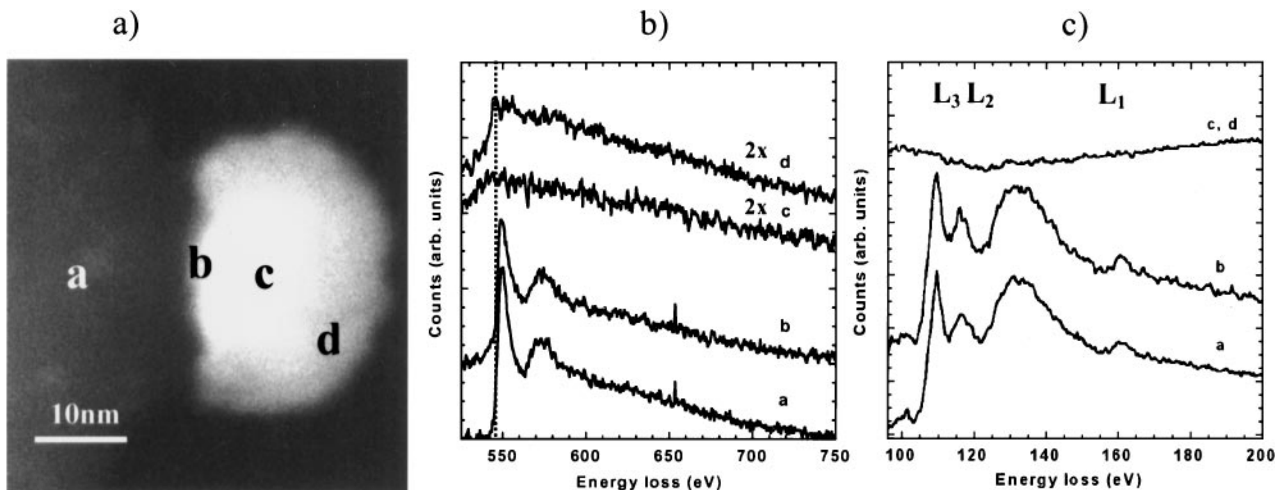

FIG. 1. Pt/SiO_2 (calc. 350°C) at room temperature: (a) Z-contrast image with locations of EELS analysis indicated; (b) EEL spectra showing O K-edges (acquisition time $t = 10$ s). The dotted lines indicate the edge onsets. Spectra c and d are magnified by a factor of 2. (c) EEL spectra showing Si L-edges with acquisition time $t = 0.3$ s.

expect to be broadened to ~0.4 nm by multiple scattering. Spectrum (a) and (b) both show an amorphous O signature with the edge onset located at 539 eV. In the Pt-particle bulk there is no contribution visible from any oxygen (spectrum c). The spectrum from the lower contrast edge shows a shift to 532 eV for the edge onset and to 546 eV for the main peak (previously at 548 eV).

The Si L-edge spectra (Fig. 1c) are taken from the same positions. The support bulk spectrum (a) displays the fine structure expected for amorphous SiO_2 (21). The edge onset is located at 105 eV, and the peaks are at 108 eV (L_3), 112 eV (L_2), and 160 eV (L_1), respectively. Although the intensity ratios differ slightly, the interface spectrum (spectrum b) exhibits the same peaks, which is attributed to the thinner illuminated edge of the SiO_2 sphere. The metal particle bulk spectrum shows no obvious modulation of the background (spectrum c). The lack of modulation in this spectrum shows that the Pt O-edge does not change the interpretation of the spectra, described in later sections. The particle surface spectrum (not displayed here) exhibits similar features as spectrum (c). This indicates an absence of silicon in or on the surface of the metallic particle.

Pt/SiO_2 (250°C)

The room temperature Z-contrast images (Fig. 2a) again show the bright core and the darker halo around the center.

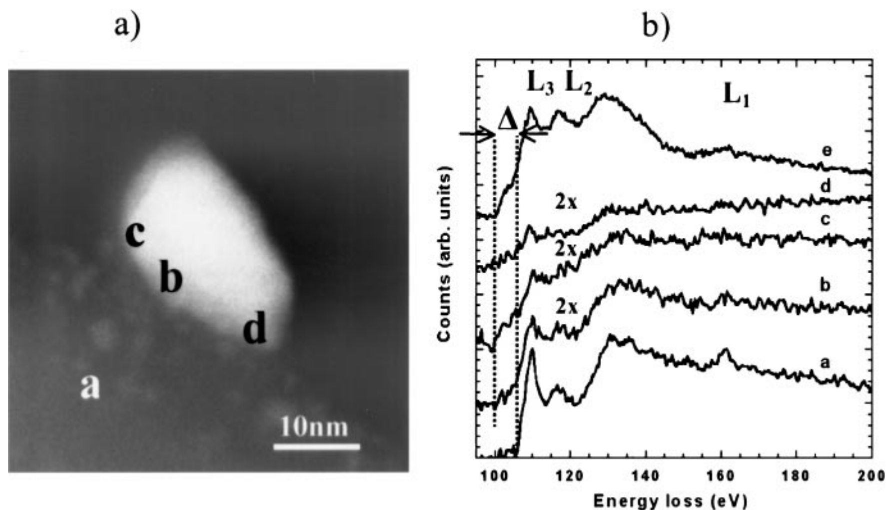

FIG. 2. Pt/SiO_2 (calc. 250°C) at room temperature: (a) Z-contrast image with locations of EELS analysis indicated. (b) EEL spectra showing Si L-edges (acquisition time $t = 0.3$ s). Spectrum e reflects a Si/SiO_2 model spectrum. The interface spectra are magnified by a factor of 2 to observe the changes in the fine-structure. The dotted lines indicated the edge onsets with an edge onset shift of $\Delta = 3.5$ eV.

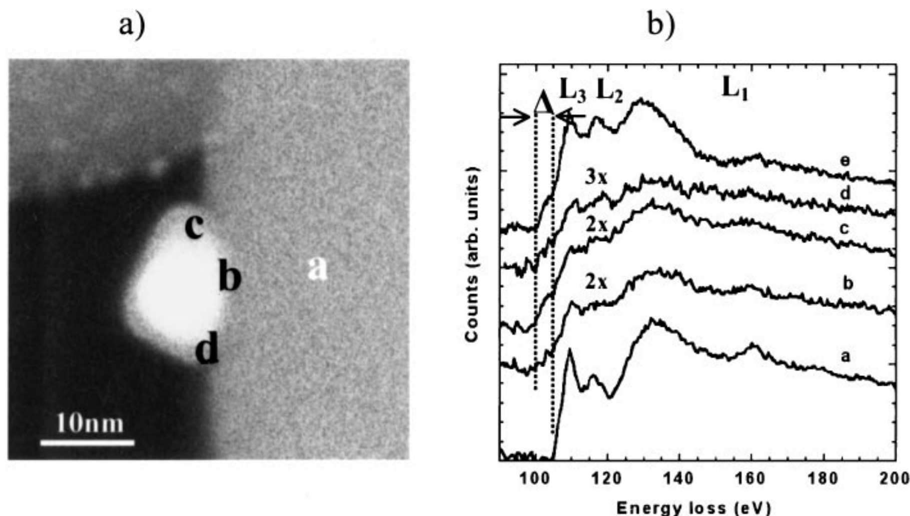

FIG. 3. Pt/SiO_2 (calc. 250°C) at 300°C after 3 h of heating: (a) Z-contrast image showing the heated metal particle and locators for EEL spectra. (b) Si L-edges from the indicated positions (dwell time $t = 0.3$ s). Spectrum e reflects a Si/SiO_2 model spectrum.

The EEL spectra (Fig. 2b) are acquired from positions as indicated in Fig. 2a. The oxygen data are not shown, because oxygen edges were only detected at the supporting oxide and the interface.

Spectrum (a) looks similar to the bulk spectrum of the amorphous support in the previous section. At the center of the heterointerface (spectrum (b)) all the Si-edges are still visible, and the peak intensity ratios are different due to the decreased specimen thickness. The edge of the interface (spectra (c)) shows a decrease in the L_1 and L_3 edge intensities and a shift in the edge onset from 105.5 to 102 eV. The energy loss spectrum from a bulk crystalline Si/SiO_2 interface from a semiconductor device viewed edge on is displayed in spectrum (e). Spectrum (c), as well as spectrum (d), shows a remarkable similarity to the reference Si/SiO_2 spectrum.

To further investigate these changes in the fine structure of the Si L-edges, the catalytic system was heated in the microscope column to a temperature of 300°C. The temperature gradient was chosen to be 10°C/min and a total stabilization time of 3 h was allowed. The structure of the particles and of the metal–oxide interface at 300°C (Fig. 3a) appears to be unchanged (i.e., no oxide skin was found at the metal clusters). The EEL spectra (Fig. 3b) exhibit pronounced changes in the fine structure of the interface Si L-edges. The SiO_2 bulk spectrum onset remains unchanged, but the spectra (b), (c), and (d) display a more substantial decrease in the L_3, L_2, and L_1 edge intensity than was previously observed. In addition to the near total disappearance of the L_3 and L_1 peaks, there is also extra intensity below this onset of the bulk spectrum. The Si–SiO_2 EEL spectrum is displayed again as (e) in Fig. 3b. To exclude beam damage as a possible formation mechanism, we acquired a series of spectra under similar conditions close to the surface of Si-spheres without any Pt-particles attached. The material remained stable under the electron beam for the dwell times used in all of this analysis.

At room temperature the Si : O intensity ratio (note that this is not the chemical composition ratio, as the scattering cross sections are not taken into account) increased from 0.9 ± 0.1 in the support to 1.2 ± 0.1 at the heterointerface, whereas at 300°C this difference is further enhanced (0.9 ± 0.1 in the support and 1.9 ± 0.1 at the interface). We also compared the integrated Si prepeak (i.e., the area under the graphs between the dotted lines) to the white line (L_3, L_2) intensities. The prepeak intensity in spectrum (b) in Fig. 2b is half of that from the reference spectrum (e). Spectra (c) and (d) show an increase in this intensity, to 1.4 and 1.1 times the reference value, respectively. The *in situ* reduced sample (Fig. 3b) exhibits an increase in the prepeak to L_3, L_2 ratio of 50% in spectrum (b) and a 12% increase in spectrum (d).

5. DISCUSSION AND CONCLUSIONS

Pt/SiO_2 (350°C)

A careful analytical approach to the results from this system reveals an unexpected location for oxygen. The combination of the oxygen and silicon near-edge fine structure analyses unambiguously show that an ordered oxide layer surrounds the Pt particles, which may be identified as PtO_x. The very low intensity of the spectral changes and the fact that these changes only occur in the surface spectra indicates that the thickness of this layer is in fact only around one or two monolayers. This structure can be explained by partial surface oxidation or chemisorption of oxygen on the Pt-metal particle during calcination at such high temperatures. Furthermore, an adsorbed layer of oxygen after calcination or due to surface contamination would not be

stable under the electron beam and not show the nearest neighbor interaction, seen in the surface oxygen spectrum (Fig. 1b, spectrum d) Hence a Pt-O surface layer seems the best explanation for the observed changes in the oxygen near edge fine structure. The fact that bulk platinum is regarded as very hard to oxidize does not contradict this observation, because small metal clusters often exhibit a completely different behavior with decreasing particle size (6). The fact that the SiO_2 directly under the interface seem not to be reduced may be explained by some passivation effect of the metal oxide skin and will be the subject of future research.

Pt/SiO$_2$ (250°C Calc.)

The monolayer of surface oxide around the Pt clusters was not observed for the sample calcined in air at 250°C (this suggests that oxidation of these Pt particles occurs at higher temperatures). However, the more interesting result in this sample is the change in the fine structure of the silicon L edges. This change can be attributed to the reduction of amorphous SiO_2 at the heterointerface. The interface spectra exhibit a very similar prepeak intensity with respect to the white line intensities as the reference Si/SiO_2 spectrum. The reduction of SiO_2 at the interface (i.e., Figs. 2b and 3b, Spectra b–d) can be attributed to the metal support interaction, similar to the one seen at SiO_2-Co interfaces (22).

Other techniques did not measure this interaction due to their lack of spatial and elemental sensitivity that is provided by the combination of Z-contrast imaging and atomic resolution EELS. Neither XAFS nor AXAFS (atomic XAFS) (7) is able to detect such small amounts of pure Si material. The fraction of reduced silica with respect to the total number of SiO_2 molecules is given by

$$N = \frac{3 \cdot \bar{l}^2 \cdot \bar{n} \cdot M_{\mathrm{SiO_2}}}{32\pi \cdot \bar{r}^3 \cdot r_{\mathrm{si}}^2 \cdot \rho_{\mathrm{SiO_2}} \cdot R}, \qquad [1]$$

where $\bar{l}$ is the average surface length, $\bar{n}$ the average particle number per supporting sphere, r_{Si} the Si atom radius, $\bar{r}$ the average SiO_2 sphere radius, $M_{\mathrm{SiO_2}}$ is SiO_2 molar weight, and R Avagadro's number. The following figures were estimated from low magnification micrographs: $\bar{r} = (103.2 \pm 12.1)$ nm, $\bar{l} = (11.2 \pm 1.2)$ nm, $\bar{n} = (0.4 \pm 0.2)$. With the given values $\rho_{\mathrm{SiO_2}} = 2.25$ g/cm^3 (for the density of glass), $M_{\mathrm{SiO_2}} = 60.1$ g/mol, and $r_{\mathrm{Si}} = 0.111$ nm, one can roughly estimate N to be (4.9 ± 2.7) ppm.

This value clearly lies below the detection limit of all conventional, low-spatial-resolution analytical methods and naturally explains why this effect has remained undetected in such a well-studied system. A possible explanation is that a thermally induced $PtSi_x$ layer, very similar to the $CoSi_x$ interface structure observed in $Co/SiO_2/Si$ (22), can build up at the heterointerface. It is further supported by the increase in the Si : O ratio at the interface, which infers lower oxygen content. Furthermore, the fact that the Si prepeak increases upon *in situ* reduction, suggests a growing amount of Si present in the interface. Careful simulations of the experimental EEL spectra, further investigations of similar systems, and the correlation of this data to other conventional results will help to solve the origin of this effect and lead to an understanding of the influence of this interface layer on the overall performance of the catalytic system.

6. CONCLUDING REMARKS

The ability to observe structure, characterize composition, and map electronic-structure changes at close to atomic resolution under various thermodynamic conditions provides an unparalleled capability to understand the effects that the interface and surface of metallic particles impose on the overall behavior of heterogeneous catalytic systems. Preliminary results from Pt/SiO_2, although not obtained from the smallest metal clusters, show the potential of these techniques to detect and locate the order of a single layer of material with atomic precision at on surface of the metal clusters as well as at the cluster–support interface. This provides an experimental method to test the prediction of conventional defect chemistry with subnanometer analytical imaging methods and to investigate materials with a sensitivity never achieved before. In the future, the combination of Z-contrast imaging and EELS in correlation with conventional methods such as chemisorption or X-ray diffraction may provide an exceptional tool for the investigation of new effects observed in these catalytic system, and achieve the long-term goal of explaining their origin.

ACKNOWLEDGMENTS

This research was sponsored by ExxonMobil Research and Engineering Company. Experimental results were obtained on the JEOL 2010F, operated by the Research Resources Center at UIC and funded by the NSF under Grant DMR-9601796. The authors thank S. Miseo and W. C. Horn from ExxonMobil Research and Engineering, NJ, for providing the catalyst samples.

REFERENCES

1. Bond, G. C., "Heterogeneous Catalysis: Principles and Applications." Oxford Science Publications, Oxford, 1987.
2. Datye, A. K., and Smith, D. J., *Catal. Rev. Sci. Eng.* **34**, 129 (1992).
3. Reuel, R. C., and Bartholomew, C. H., *J. Catal.* **85**, 78 (1984).
4. Pennycook, S. J., and Boatner, L. A., *Nature* **366**, 143 (1993).
5. Browning, N. D., Chrisholm, M. F., and Pennycook, S. J., *Nature* **366**, 143 (1993).
6. Taylor, K. C., *Catal. Rev. Sci. Eng.* **35**, 457 (1993).
7. Mojet, B. L., Miller, J. T., Ramaker, D. E., and Koningsberger, D. C., *J. Catal.* **186**, 373 (1999).
8. Somorjai, G. A., and Rupprechter, G., *J. Phys. Chem.* **103**, 1623–1638 (1999).
9. Vannice, M. A., and Poondi, D., *J. Catal.* **169**, 166 (1997).

10. Bernal, S., Botana, F. J., Calvino, J. J., Cifredo, G. A., Garcia, R., and Rodrigues-Izquierdo, J. M., *Ultramicroscopy* **34**, 60 (1990).
11. Nellist, P. D., and Pennycook, S. J., *Science* **274**, 413 (1996).
12. Disko, M. M., Ahn, C. C., and Fultz, B., “Transmission Electron Energy Loss Spectrometry in Materials Science.” The Minerals, Metals & Materials Society, 1992.
13. Egerton, R. F., “Electron Energy Loss Spectroscopy in the Electron Microscope.” Plenum, New York, 1986.
14. James, E. M. and Browning, N. D., *Ultramicroscopy* **78**, 125 (1999).
15. James, E. M., Browning, N. D., Nicholls, A. W., Kawasaki, M., Xin, Y., and Stemmer, S., *J. Electron Micross.* **47**(6), 561 (1998).
16. Nellist, P. D., and Pennycook, S. J., *Ultramicroscopy* **78**, 111 (1999).
17. Jesson, D. E., and Pennycook, S. J., *Proc. R. Soc. London Ser. A* **449**, 273 (1995).
18. Fertig, J., and Rose, H., *Optik* **59**, 407 (1981).
19. Pennycook, S. J., Jesson, D. E., and Browning, N. D., *Nucl Instrum Methods B* **96**, 575 (1995).
20. Klie, R. F., Ito, Y., Stemmer, S., and Browning, N. D., *Ultramicroscopy* **86**, 289 (2001).
21. Batson, P. E., *Nature* **366**, 727 (1993).
22. Kurmaev, E. Z., Shamin, S. N., Galakhov, V. R., and Kasko, I., *Thin Solid Films* **311**, 28 (1997).